ISSN: 1992-8645 www.jatit.org E-ISSN: 1817-3195

ENSEMBLE FEATURE EXTRACTION MODEL WITH OPTIMAL KERNELIZED CLUSTERING ALGORITHM FOR IDENTIFYING THE CANCER FROM CERVICAL HISTOPATHOLOGY IMAGES

BAGHIALAXMI R[1], DR. KIRUBAGARI B[2], DR. LAKSHMANA PANDIAN S[3]

[1]Research Scholar, Department of CSE, Annamalai University, India

[2] Associate Professor, Department of CSEFEAT, Annamalai University, India

[3]Associate Professor, Department of CSE, Puducherry Technological University, India

E-mail: [1]laxmiram1995@gmail.com, [2]kirubacdm@gmail.com, [3]lpandian72@pec.edu

ABSTRACT

Cervical cancer, a disease that affects women the most. When a woman's cervix undergoes some modifications, this is visible. These cancer cells have the ability to spread to another parts, including bladder, livers, lungs, rectum, further complicating situations. Higher rates of recovery have been reported with earlier discovery, screening, and rigorous procedures. This paper proposes a novel technique to detect cervical cancer utilizing deep learning techniques. The idea is to provide improvement in the efficiency, the network used to cluster the images using Optimal Kernelized Fuzzy C-Means (OKFCM) clustering along with classified image to give high-resolution image classification.Then to build an accurate cervical cancer histopathological image ensemble based feature extraction model, which is the very first and most important procedure in our system. An artificial neural network is used to distinguish between normal, abnormaland malignant cells, producing accurate findings than manual testing procedures like Pap test and LBC (Liquid Based cytology). Database of 962histopathological cervicalimages used to test our technique.The outcomes of all trials proved that this technique produced the best results inPrecision, Specificity,Recall, AUC,Accuracy, FPR and FNR. This strategy can help pathologists with cervical disease categorization by reducing their cognitive load and increasing their diagnostic efficiency and accuracy. It will have the ability to be used in medical care for the diagnosis of cervical cancer histology.

Keywords: *Cervical Cancer, Deep Learning, Classification, Feature Extraction, Histopathological Image*

1. INTRODUCTION

Since the previous several decades, cervical cancer has been a leading cause of mortality globally. Among the cancer caused in women, it takes the third place, behind lung and breast cancer. It can only be cured on earlier diagnosis and provided treatment. This stage refers to the progression and spread of cancer in a woman's body. After a diagnostic test, doctors can determine the stage of cancer. Physicians can follow the suitable form of treatment if they know the exact stage of cervical cancer. The FIGO has developed four phases of cervical cancer[1]. The stage is determined by a doctor's assessment of the tumor and its spread to lymph nodes or other regions of the body. According to research, irregular bleeding between or after menopause, abnormal vaginal discharge, exhaustion and weight loss, discomfort in the pelvis and abdomen, and irritation when peeing are the six fundamental signs of cervical cancer. Long-term infection and infection with the human papillomavirus are the two primary causes of cervical cancer infection (HPV). The presence of aberrant cells at the cervix wall promotes the growth of cancer cells and tumors. HPV damages skin cells and mucous cells, causing aberrant behavior that can lead to pre-cancerous conditions and eventually, cervical cancer stage I [2]. Women who smoke, have a weakened immune system, are HIV-positive, and/or they have had an organ transplant at the highest risk of contracting cervical cancer than others. According to the NCBI, over 96000 women in India get infected with cervical cancer each year, with approximately forty percentage of them dying as a result. The majority of these ladies are between the ages of thirty and sixty nine. After a physical examination or pap test smear findings, gynecologists believe that swelling around the womb or within the vagina increases the risk of cervical cancer.They use a colposcopy to look at the changes in the tissues (kind of magnifying glass). Other examination methods, such as ultrasound, CT Scan,MRI and X-ray, may be required to evaluate the infection at deeper levels depending on the degree of infection detected during the physical examination. Cervical cancer is diagnosed using a standard approach [3]. Cervicographytesting, external expert readers read morphological anomalies of the cervix after adding five percentage acetic acid and then the cervix uptomaximum50 times using a camera ismagnified[4]. This procedure had a drawback that it necessitates, the significant material resources and human resources, as proper cervical dilatation test'sreading necessitates the use of a professional reader with an international reading license. Furthermore, because there may be inter-intra observer mistakes, it is critical to improve objectivity by controlling the quality of regular and systematic reader. The reader's subjective opinion in cervical reading and the researcher's health status may influence the outcomes. Computer-aided technologies for diagnosis, like traditionalMLand DL. High-level notion of DLis ML that denotes a set of procedures for analyzing and learning data and making judgments depending on that data [5]. Artificial Neural Networks (ANN) are included with ML like the structure of human brain. The value of gradient is converged to zero and the local maximum is dropped so that an artificial neural network cannot learn or handle new input. And, utilizing pre-learning and dropout approaches known as DL, DL is strapped beyond the boundaries of the existing ANN[6].

High Squamous Intra-Epithelial Lesion means a sexual transmission which was before illness resulting from infections with Human Papilloma virus (HPV). After the infection spreads the specialised squamous cells on the cervix's surface.Low Squamous Intra-Epithelial Lesion means Squamous cells make up the layer that surrounds the cervix. Cervical cancer, pre-cancer and various irregularities of the cervical cells are all detected.Negative for Intra-Epithelial Malignancy means no cancer cells or other abnormal cells have been found on the surface or in the tissue that lines the cervix. Squamous Cell Carcinoma means Skin cancer which originates inside the Squamous cells that form the central and outside layers of the skin.

1.1 The Contribution of this Paper

- To build an accurate cervical cancer histopathological image ensemble based feature extraction model, which is the very first and most important procedure in our system.
- To improve the efficiency, the network used to cluster the images using Optimal Kernelized Fuzzy C-Means (OKFCM) clustering along with classified image to give high-resolution image classification.
- The bigger the number of process able features, the more features are acquired based on the pre-processed picture, which are then further processed to obtain features that are not redundant.

The paper is arranged as follows section 2 describes the related works on cervical cancer feature extraction and classification. The system model is explained in detail in section 3. The section 4 analyzes the performance measures and the conclusion is explained in section 5.

2. RELATED WORKS

Machine learning methods were used, and its segmentation refinement was compared to a classifier of cervical cancer, with random forests producing better results [7]. Adaboost detectors [8], Support vector machine [9], and Gaussian mixture models [10] have also been employed for managing supervised learning techniques to the varied picture or super pixel patches from objects extracted[11]. The multi filter SVM was run, and the parameters for identifying cervical cells were established. ANN were used to build and evaluate cervical cell categorization with an accuracy of 78 percent [12]. An unsupervised strategy was used to handle unbalanced medical evidence for a range of cervical cancers with no parameter changes[13]. All other fundamental classification models were surpassed by particle swarm optimization using K-Nearest Neighbors values of membership[14]. Form and texture features of classification and segmentation approach, as well as Gabor properties, utilized for classifying cervical cancer cells. Both normal and cancer cell categorization were shown to have a superior accuracy of 89 percent [15]. The least square support vector machine (LSSVM) was used to classify the retrieved features from CNN, and it generated more impressive results, making it one of the proposed model's reference components [16]. SVM based on the radial basis function (RBF) also performed well, outperforming logistic regression and random forest approaches [17]. The accuracies were found to vary from 90 to 95 percent based on the characteristics. DL architectures including ResNet, tree models and Inception [18] shows a promise in a variety of applications, including cancer cell detection. A successful kind of deep learning technique is Convolutional neural networks that is often utilized for detecting and recognizing the cervical cancer [19]. To extract deep learning characteristics from cervical pictures, a technique based on CNNs was developed for earlier detection classification of cervical cancer cell[20]. The input images are categorized by using extreme learning machine (ELM). For transfer learning and fine-tuning, the CNN paradigm was applied. Alternatives to the ELM, the Automobile Encoder (AE) classifiers and the multilayered Perceptron (MLP)were investigated [21]. In order to balance the number of instances in the dataset, CCPM first removes outliers by utilizing outlier detection approaches like Density-Based Spatial Noise Cluster and isolation Forest. This method has demonstrated to be more accurate in predicting cervical cancer. The scientists created a novel Regionally Growing Extraction Function for extracting information of diagnosisfrom pictures [22].

In the existing models, the feature extraction task is studied in a limited way on manually cropped cancerous regions whereas a fully automated application necessitates computationally expensive in whole slide medical image processing. It produces a significant amount of feature information.To propose an Ensemble DL framework withnew techniques and methods for preprocessing, clustering, feature extraction, classification process for histopathological cervical biopsy images and to present an optimum kernel based fuzzy c means (OKFCM) technique to overcome the limitations. In section 3 a new model is introduced in order to remove the limitations.

3. SYSTEM MODEL

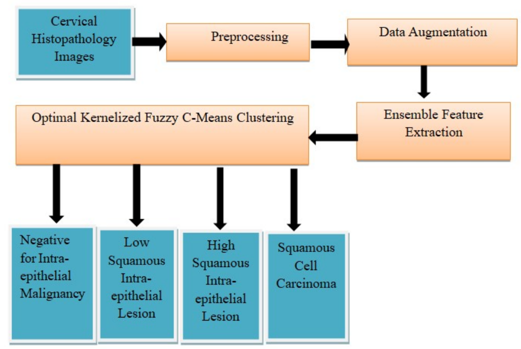

Figure 1: Proposed Architecture

This section discuss about the Proposed Feature Extraction technique in Cervical Cancer Detection for Histopathological Images. The Cervical Histopathology images are preprocessed using Adaptive median filter, Macenko-stain Normalization to remove unwanted noise. Pre-normalization is done to enhance the clarity of image. The Data Augmentation makes the preprocessed image to be de-texturized, de-colorized, edge enhanced, flip and rotate. The augmented image then undergoes to feature extraction process. The augmented image is given for feature extraction by using ensemble based method such as Resnet, Resboltz, Alexnet. Optimal Kernelized Fuzzy C-Means clustering method is classified using four classes i.e., NILM, SCC, LSIL and HSIL to optimize the results. The proposed Architecture is shown in Figure 1.

3.1 Pre-Processing

Step 1: The Histopathological cervical images taken is about 962 images from 460 samples from the normal and abnormal patient is used as an input size is 2048x 1536 pixels then itresized.

Step 2: RGB image is converted to HSV color scale image.

Step 3: Adaptive median filter is applied to the HSV color scale image.

Step 4: Then Macenko-stain normalization is appliedon the HSV color scale image.

Step 5: The final output of the pre-processing stage is the pre-processed cervical image.

3.2 Adaptive Median Filtering

Step 1: Create a WW-sized sub-window around the current pixel, where W=3.

Step 2: Determine if the difference between the highest and lowest pixel value under consideration in the window is more than a threshold value of Edge Detect (0.0, 0.1),VerticalFlip (0.5),Rotate (-25, -25) and Horizontal Flip (0.5); if not, continue on to the next pixel and repeat step 1.

Step 3: Locate any pixels in the sub-window that are not part of the highest or lowest value.

Step 4: If the number of such pixels (excluding the minimum and maximum) is higher or equal to W, compute the median of the pixels that are not included of the highest and lowest value; otherwise (else), expand the window size by W=W+2 and return to step 1.

Step 5: If the present pixel's highest and lowest values are identical, substitute it with the omitted median value; if (otherwise), leave it alone and go to step 1.

3.3 Macenko-Stain Normalization

By calculating the staining vector and then normalising the staining intensity, the MacenkocolourNormalisation approach converts the pictures to a staining colour space. Color information can be more reliably manipulated by quantifying the stain colour vectors (each stain's RGB contribution). Nevertheless, because of the staining's unpredictability, an automatic approach for determining staining vectors is recommended. Macenko uses pictures in the Optical Density space to build an automated stain vector synthesis approach. The OD values obtained are the outcome of a linear transformation of the staining vectors. Because backdrop has an OD of 0, lower OD measurements are threshold to optimize performance. A single value decomposition (SVD) is used to get the biggest OD values.The biggest optimum value are used to create a plane, and the remaining OD pixels are projected onto it with their vector lengths normalized to unit length. Each point's angle with regard to the 1ststaining vector is computed. The 1st and 99th percentile rank of pixel for every value are utilized to correct for distortion and guarantee that the extremities are genuine. After that, the extremities are transformed back to OD space. Intensity fluctuation is compensated for every stain. To accommodate for disturbance, an intensity histogram is shown with the 99th percentile as the peak. The staining intensity histograms in the target picture are then adjusted to the original maxima.

3.4 Data Augmentation

Data augmentation is a technique for expanding trained method by analyzing modifications and deflections on labelled data, given rise to new samples that may be used as extra training information. The labels stay unaltered after modifications are applied, which is an important feature of data augmentation. Crop, revolutions, translates, sizing and duplicating of labelled samples are all examples of data augmentation. Supplementing information during the training phase has been found to increase the model's exclusionary and adaptation abilities.

3.5 Ensemble Feature Extraction using ResNet, ResBoltz, AlexNet

This section discusses about the proposed Ensemble Feature Extraction Architecture using ResNet, ResBoltz and Alexnet.

Residual units form the basis for deep residual networks as shown in Figure 2. Every residual unit will becalculated in equation (1) as

$$y_i = h(x_i) + F(x_i, w_i); \; x_{i+1} = f(y_i) \quad (1)$$

Where, a residual function is given byF, ReLU function is denoted by f, the weight matrix is represented by$w_i$and $x_i$is the i^{th} layer's outputs and $y_i$is the i^{th} layer's outputs.

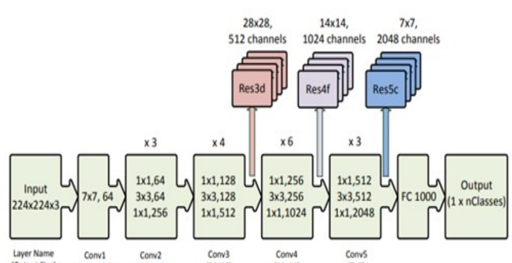

Figure 2: ResNet-based Feature Extraction

The h function is an identity mapping expressed in equation (2) as

$$h(x_i) = x_i \tag{2}$$

Definition for the residual function F is given in equation (3),

$$F(x_i, w_i) = w_i \cdot \sigma\left(B(w_i') \cdot \sigma\left(B(x_i)\right)\right) \tag{3}$$

Wherethe Batch Normalization is represented by B(x_i)convolution is denoted by "·" and max(x, 0)=σ(x). Path branching for propagation of gradient is the necessary idea scheduled behind the residual learning.

A bipartite graph having a pair of layers is comprised in Restricted Boltzmann (ResBoltz) as shown in Figure 3. Hidden units $h \in \{0,1\}^P$and Visible units$v \in \{0,1\}_i^D$ are comprised in it while each visible unit is related to each and every hidden units by weight matrix whereas, there no connection of units is present inside the same layer.

TheRBM's parameters will be learnt by the likelihood maximization. The log-likelihood's derivative is expressed in equation (4)

$$\frac{\partial}{\partial\theta}L(\theta) = -\left\langle\frac{\partial E(v;\theta)}{\partial\theta}\right\rangle_{data} + \left\langle\frac{\partial E(v;\theta)}{\partial\theta}\right\rangle_{model} \tag{4}$$

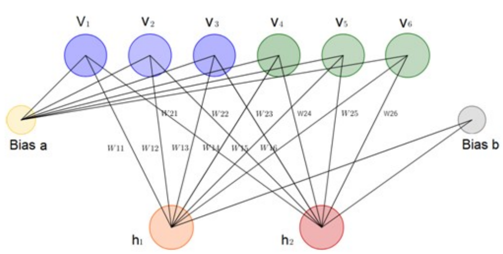

Figure 3: ResBoltz Architecture

Where RBM'sfree energy function is provided with ∂E (v; θ) and the visible vector v's expected values as per the data and model is represented by data and model convolution. But, the expected value computation are difficult as numerous Exponentialterms are involved it. The two adjacent layers are established with connections and there is no connection establishment between the same layer units among each other. The layer wise strategy is used for learning DBNparameters.

The Eight Layer Convolutional neural network is AlexNet, which consists five Convolutional Layer and three full connection layers. After the 3 Convolutional layers, the maximum pooling operation is carried out and it is shown in Figure 4.

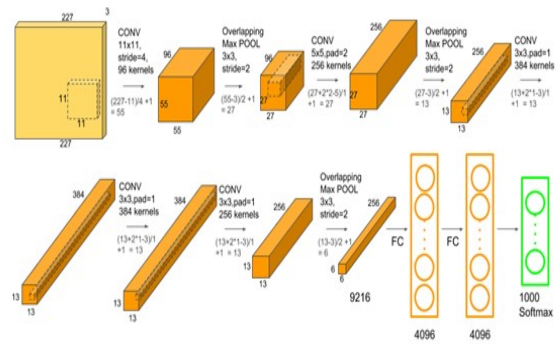

Figure 4: AlexNet Architecture

As compared to existing neural networks, AlexNet is different, as it uses the activation functionReLU rather than Tanh and conventional sigmoid functions. This model's training speed is not only improved by ReLU and gradient explosionhas it controlled gradient disappearance problems. Deeper networks are easily trained by ReLU. ThefunctionReLU is represented in equation (5),

$$\text{ReLU}(x) = \max(0, x) \tag{5}$$

The over fitting degree (Model's process of training) is reduced by using dropout in AlexNet, in certain probability, neurons are stopped, therefore the local node dependencies are lowered and the model's ability of generalization is enhanced [16].

3.6 Optimal Kernelized Fuzzy C-Means Clustering Method:

The kernel trick forms the basis for the kernel method algorithms and it is as follows:non-linear map is used from the data space to the feature mapped space, a dataset $\Phi X \rightarrow F_x \rightarrow \Phi(x)$ where X€$\{x_1 \ldots, x_n\}$(an input data space with low-dimension), which is potentially mapped into feature space of higher-dimension or F as inner producthaving tuned goal of original problem of non-linearity in the potential input space.

S= $x_1, x_2 \ldots x_m$ as m samples. m × m matrix is K, includes inner products amongeach and every pairs of instances, i.e., k_{ij}=k(x_i,x_j). $K_{ij} = k(x^\wedge i, x^\wedge j)$ K is symmetric asΦ (x). Φ (y) =k(x, y) = k(y, x)function is a kernel if the kernel matrix for each finite sample S is positive semi-definite. In the following, the input dataΦX_i, where i=1,2.., is employed to make it feasible using Mercer kernels. N is the number of dimensions in the feature space of high-dimension. Φ(X_j) where j=1,2…., M, where the nonlinear mapping function is defined as Φ (.).

The OKFCM technique augments the classic fuzzy c-means algorithm with kernel information, overcoming the FCM algorithm's inability to handle tiny variations across clusters. Theinput data spaceis convertedbykernel approach in nonlinear way. A Mercer kernel produces Rq asan implicit function space, according to the Mercer theorem. In the kernel K’sfeature space, the Euclidian distance among samplesX_i and X_j may be defined in equation (6) as follows:

$$d_{ij} = \text{dist}\left(\phi(X_i), \phi(X_j)\right) = \sqrt{\left\|\phi(X_i) - \phi(X_j)\right\|^2} \tag{6}$$

Distances are directly calculated from kernel function.

$$\mathrm{d_{ij}} = \sqrt{\Phi(X_i)\Phi(X_j) - 2\Phi(X_i)\Phi(X_j) + \Phi(X_j)\Phi(X_j)} = \sqrt{K(X_i)K(X_i) - 2K(X_i,X_j) + K(X_j)K(X_j)} = \sqrt{2 - 2K(X_i - X_j)} \tag{7}$$

Depending on the FCM algorithm, the J_{km}object function is defined as:

$$J_{km} = 2\sum_{j=1}^{c}\sum_{i=1}^{N} U_{ij}^{m}\left(1 - K(X_i, W_j)\right) \tag{8}$$

$$U_{ij} = \frac{\left(1-K(X_i W_j)\right)1/(m-1)}{\sum_{k=1}^{c}\left(1-K(X_i,W_K)\right)/(m-1)} \tag{9}$$

As perequation (7), (8) and (9),equation (10) is minimized by using Lagrangian optimization previously, the$W_j$is thenew iterative center and membership and update equation is represented byU_{ij}.

$$W_j = \frac{\sum_{i=1}^{n} U_{ij}^{m} K(X_i, W_j) X_i}{\sum_{i=1}^{n} U_{ij}^{m} K(X_i, W_j)} \tag{10}$$

4. PERFORMANCE ANALYSIS

The Implementation of the proposed feature extraction and classification is done using Python tool and the configurations considered for the experimentation are: PC with Windows 10 pro, 8GB RAM, and Intel i3 processor CPU @1.70GHz, 64 bit operating system.

The Kaggle dataset is used for deriving the experimental data. The dataset of Colposcopy cervical cancer is divided into Eighty percentage,Ten percentageand Ten percentage for training, testing and validation respectively. The numberof epoch used to trainthe model is 50. The multi-GPU environment, 0.0001 as therate ofinitial learning, the batch of size is 64 used for training.

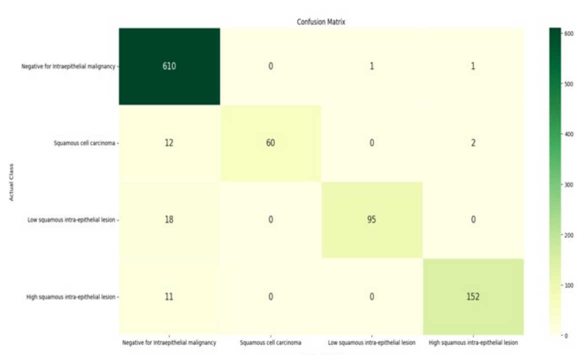

Figure 5: Confusion Matrix of Proposed Technique

The OKFCM of the proposed method is given in Figure 5. Based on this confusion matrix the cancer cells have been extracted. The actual class and predicted class of input image of the tumor cells has been analyzed based NILM, SCC, LSIL and HSIL. Here, multi-class classification of many classes C_i. t_{pi} represents true-positive class means a result that correctly indicates the presence of a cancer ;f_{pi} represents false-positive class means a result which is

Journal of Theoretical and Applied Information Technology
15th July 2022. Vol.100. No 13

ISSN: 1992-8645 www.jatit.org E-ISSN: 1817-3195

wrongly indicates that a particular cancer is present; t_{ni} represents true-negative class means a result that correctly indicates the absence of a cancer ;f_{ni} represents false-negative class means a result which is wrongly indicates that a particular cancer is absent.The metrics considered for estimating the efficiency of the proposed model are Precision, Specificity, Recall, AUC,Accuracy, FPR and FNR.

Table 1 shows the various classes of input images and their output images. Based on pre-processing, augmentation and finally extracted images are classified. The processing of input image has been analyzed based on classes of tumor as NILM, SCC, LSIL and HSIL. For these classes of Tumorcells the input images has been taken, pre-processed, augmented and classified and final output will be classified image of all these Tumor classes.

The result analysis of the proposed shows better performance in using Adaptive Median Filter, Macenko-Stain Normalization and then by using Resnet, Resboltz, Alexnet. Optimal Kernelized Fuzzy C-Means clustering method into four classes to optimize the output with higher efficiency.

Table 1: Various Classes of Input and Output Images

Classes	Input Images	Pre-Processed	Augmentation	Output Images
High Squamous Intra-Epithelial Lesion	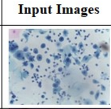	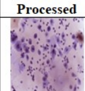	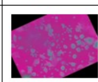	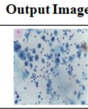
Low Squamous Intra-Epithelial Lesion	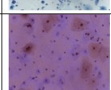	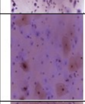	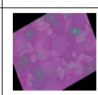	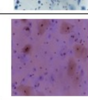
Negative for Intraepithelial Malignancy	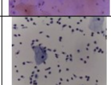	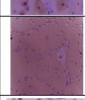	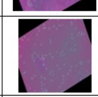	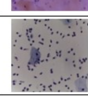
Squamous cell carcinoma	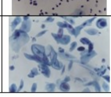	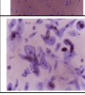	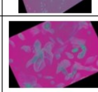	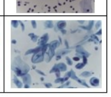

Accuracy calculate the efficiency of prediction for individual classifiers for each classes as

$$Accuracy = \frac{t_{pi} + t_{ni}}{t_{pi} + t_{ni} + f_{pi} + f_{ni}}$$

Precision is the ratio of True Positive which is correct Real Positives and is defined as

$$Precision = \frac{t_{pi}}{t_{pi} + f_{pi}}$$

Recall is the proportion of the Real Positives to the correctly Predicted Positives given by

$$Recall = \frac{t_{pi}}{t_{pi} + f_{ni}}$$

Specificitycalculate the efficiency of individual classifiers for identifying negative labels as

$$Specificity = \frac{t_{ni}}{t_{ni} + f_{pi}}$$

False positive ratecalculate theefficiency of individual classifiers for identifying false positive labels as

$$FPR = \frac{f_{pi}}{f_{pi} + t_{ni}}$$

False negative ratecalculate the efficiency of individual classifiers for identifying false-negative labels as

$$FNR = \frac{f_{ni}}{f_{ni} + t_{pi}}$$

Area under curvecalculate theeffectiveness for individual classifiers to avoid the false classification as

$$Area\ under\ curve = ½(\frac{t_{pi}}{t_{pi} + t_{ni}} + \frac{t_{ni}}{t_{ni} + f_{pi}})$$

Table2 shows the accuracy analysis for proposed technique. The input images are the Histopathological images. Proposed techniqueobtain95.9% of accuracy in 500 Epochs, 95.6% at 400 Epochs, 95.2% at 300 Epochs, 94.8% at 200 Epochs and 94.3% at 100 Epochs by the various stages of images. These values are represented graphically in Figure6.The performance measures of various techniques of existing techniques are compared with the proposed techniques in Table 2 among the values the proposed method gives better performance as shown in Figure 6.

Table 2: Comparison of Accuracy of a various Feature Extraction

ISSN: 1992-8645 www.jatit.org E-ISSN: 1817-3195

Method

Number of Epochs	AlexNet	VGG-16	VGG-19	Resnet-50	Resnet-101	Google net	Ensemble	Proposed
100	81	81.3	81.5	86.2	88.1	84.9	92.6	94.3
200	82.6	83.1	83.2	86.7	88.6	85.4	92.9	94.8
300	84	84.3	84.6	88.1	89.3	86.3	93.2	95.2
400	84.5	84.9	85.1	88.5	89.6	86.6	93.9	95.6
500	85.1	85.2	85.3	88.8	89.9	87.1	94.1	95.9

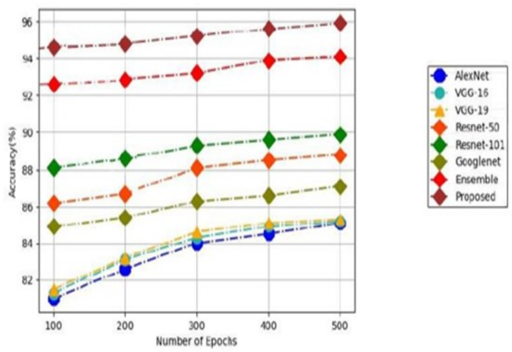

Figure 6: Comparison of Accuracy

Figure 6 shows the Comparison of Accuracyof other method which shows that the proposed method gives maximum accuracy in 500 epochs.

Table 3 shows the precisionanalysis for proposed technique. The input images are the Histopathological images. Proposed technique obtain97.9% of precision in 500 Epochs, 97.5% at 400 Epochs, 97.14% at 300 Epochs, 96.9% at 200 Epochs and 96.4% at 100 Epochs by the various stages of images. These values are represented graphically in Figure 7. The performance measures of various techniques of existing techniques are compared with the proposed techniques in Table 3 among the values the proposed method gives better performance as shown in Figure 7.

Table 3: Comparison of Precision of a various Feature Extraction Method

Number of Epochs	AlexNet	VGG-16	VGG-19	Resnet-50	Resnet-101	Google net	Ensemble	Proposed
100	79.4	81	84.6	85.7	83.4	84.6	85.4	96.4
200	79.6	81.7	85	86.1	83.8	84.9	85.9	96.9
300	80	82	85.3	86.4	84.1	85.2	86.3	97.14
400	80.5	82.5	85.9	86.9	84.6	85.6	86.9	97.5
500	80.9	83.1	86.1	87.2	84.9	85.9	87.2	97.9

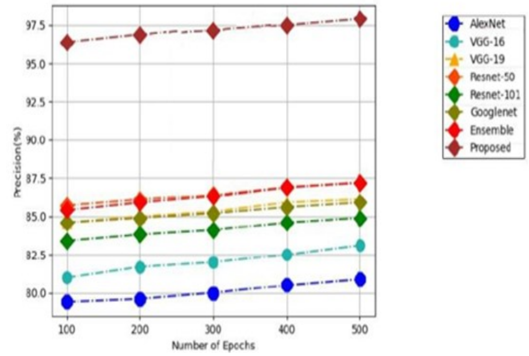

Figure7: Comparison of Precision

Figure 7 shows the Comparison of Precision of other method which shows that the proposed method gives maximum precision in 300 epochs.

Table 4 shows the recallanalysis for proposed technique. The input images are the Histopathological images. Proposed technique obtain95.9% of recall in 500 Epochs, 95.6% at 400 Epochs, 95.2% at 300 Epochs, 94.9% at 200 Epochs and 94.2% at 100 Epochs by the various stages of images. These values are represented graphically in Figure 8. The performance measures of various techniques of existing techniques are compared with the proposed techniques in Table 4 among the values the proposed method gives better performance as shown in Figure 8.

Table 4: Comparison of Recall of a various Feature Extraction Method

Number of Epochs	AlexNet	VGG-16	VGG-19	Resnet-50	Resnet-101	Google net	Ensemble	Proposed
100	80.4	79.2	81.6	85.9	86.5	87.5	86.1	94.2
200	80.9	79.6	81.9	86.1	86.9	87.9	86.5	94.9
300	81.2	80.4	83.2	86.3	87.1	88.1	87.5	95.2
400	81.6	80.9	83.6	86.9	87.6	88.5	87.9	95.6
500	81.9	81.2	83.9	87.1	88.1	88.9	88.1	95.9

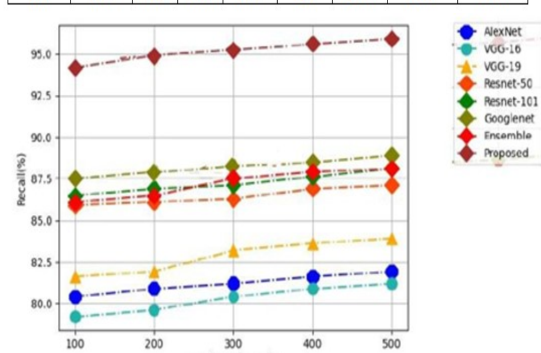

Figure 8: Comparison of Recall

Journal of Theoretical and Applied Information Technology
15th July 2022. Vol.100. No 13

ISSN: 1992-8645 www.jatit.org E-ISSN: 1817-3195

Figure 8 shows the Comparison of recallof other method which shows that the proposed method gives maximum recall in 500 epochs.

Table5 shows the specificityanalysis for proposed technique.The input images are the Histopathological images. Proposed technique obtain98.9% of specificity in 500 Epochs, 98.6% at 400 Epochs, 98.4% at 300 Epochs, 98.2% at 200 Epochs and 97.9% at 100 Epochs by the various stages of images. These values are represented graphically in Figure 9. The performance measures of various techniques of existing techniques are compared with the proposed techniques in Table 5 among the values the proposed method gives better performance as shown in Figure 9.

Table 5: Comparison of Specificity of a various Feature Extraction Method

Number of Epochs	AlexNet	VGG -16	VGG -19	Resnet-50	Resnet-101	Google net	Ensemble	Proposed
100	81.6	80.1	78.1	85.1	87.2	85.9	86.5	97.9
200	81.9	80.5	78.6	85.5	87.9	86.2	86.9	98.2
300	82.3	81.4	79.4	86.4	88.4	86.5	87.2	98.4
400	82.6	81.9	79.9	86.9	88.6	86.9	87.6	98.6
500	82.9	82.1	80.2	87.2	88.9	87.2	87.9	98.9

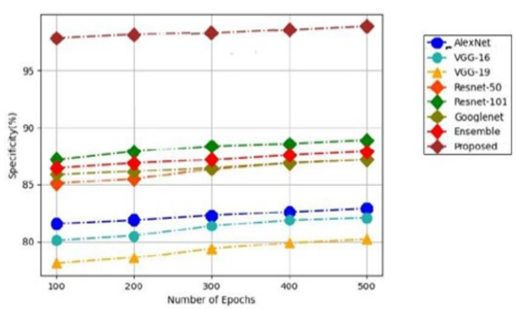

Figure 9: Comparison of Specificity

Figure 9 shows the Comparison of specificityof other method which shows that the proposed method gives maximum specificity in 500 epochs.

Table 6 shows the FPRanalysis for proposed technique. The input images are the Histopathological images. Proposed technique obtain0.017 of FPR in 500 Epochs, 0.016 at 400 Epochs, 0.015 at 300 Epochs, 0.014 at 200 Epochs and 0.013 at 100 Epochs by the various stages of images. These values are represented graphically in Figure 10. The performance measures of various techniques of existing techniques are compared with the proposed techniques in Table 6 among the values the proposed method gives better performance as shown in Figure 10.

Table6: Comparison of FPR of a various Feature Extraction Method

Number of Epochs	AlexNet	VGG -16	VGG -19	Resnet-50	Resnet-101	Google net	Ensemble	Proposed
100	0.25	0.35	0.12	0.018	0.019	0.07	0.05	0.013
200	0.29	0.37	0.14	0.019	0.019	0.09	0.07	0.014
300	0.31	0.38	0.15	0.1	0.1	0.1	0.1	0.015
400	0.33	0.41	0.18	0.12	0.11	0.13	0.15	0.016
500	0.35	0.45	0.21	0.14	0.15	0.15	0.18	0.017

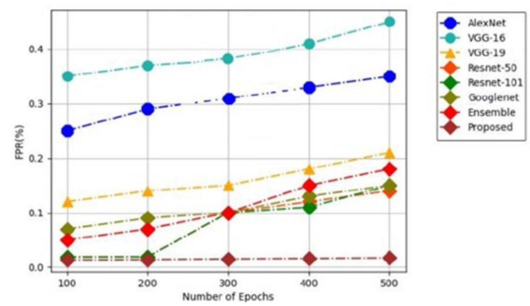

Figure 10: Comparison of FPR

Figure 10 shows the Comparison of FPR of other method which shows that the proposed method gives maximum FPR in 100 epochs.

Table7 shows the FNRanalysis for proposed technique. The input images are the Histopathological images. Proposed technique obtain0.051 of FNR in 500 Epochs, 0.049 at 400 Epochs, 0.047 at 300 Epochs, 0.045 at 200 Epochs and 0.043 at 100 Epochs by the various stages of images. These values are represented graphically in Figure 11. The performance measures of various techniques of existing techniques are compared with the proposed techniques in Table 7 among the values the proposed method gives better performance as shown in Figure 11.

Table 7: Comparison of FNR of a various Feature Extraction Method

Number of Epochs	AlexNet	VGG -16	VGG -19	Resnet-50	Resnet-101	Google net	Ensemble	Proposed
100	0.13	0.21	0.09	0.10	0.11	0.12	0.11	0.043
200	0.15	0.22	0.10	0.11	0.12	0.13	0.12	0.045
300	0.18	0.23	0.11	0.13	0.13	0.13	0.13	0.047
400	0.20	0.24	0.13	0.14	0.15	0.14	0.15	0.049
500	0.21	0.25	0.14	0.16	0.16	0.15	0.17	0.051

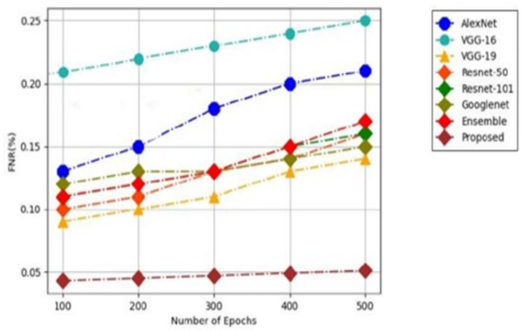

Figure 11: Comparison of FNR

Figure 11 shows the Comparison of FNRof other method which shows that the proposed method gives maximum FNR in 100 epochs.

Table 8 shows the AUCanalysis for proposed technique. The input images are the Histopathological images. Proposed technique obtain93.9% of AUC in 500 Epochs, 93.5% at 400 Epochs, 93.3% at 300 Epochs, 92.6% at 200 Epochs and 92.1% at 100 Epochs by the various stages of images. These values are represented graphically in Figure 12. The performance measures of various techniques of existing techniques are compared with the proposed techniques in Table 8 among the values the proposed method gives better performance as shown in Figure 12. It shows the Comparison of AUCof other method which shows that the proposed method gives maximum AUC in 500 epochs.

Table 8: Comparison of AUC of a various Feature Extraction Method

Number of Epochs	AlexNet	VGG -16	VGG -19	Resnet -50	Resnet -101	Google net	Ensemble	Proposed
100	69.5	72.5	79.5	80.2	85.4	86.1	88.4	92.1
200	69.9	72.6	79.9	80.6	85.6	86.5	88.6	92.6
300	70	73	80	81	86	87	89	93.33
400	70.2	73.1	80.2	81.4	86.3	87.3	89.2	93.5
500	70.6	73.9	80.5	81.6	86.5	87.7	89.5	93.9

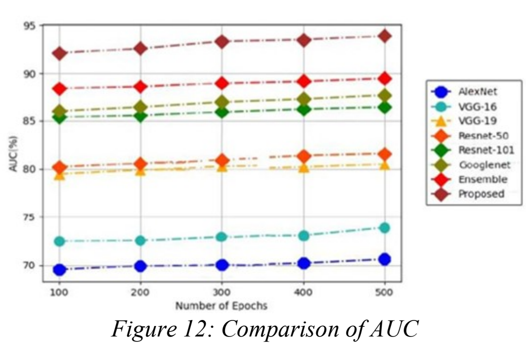

Figure 12: Comparison of AUC

Table 9: Parametric Comparative Analysis between Proposed and Existing Technique

Parameters	AlexNet	VGG -16	VGG -19	Resnet- 50	Resnet- 101	Google net	Ensemble	Proposed
Accuracy	84	84.3	84.6	88.1	89.3	86.3	93.2	95.2
Precision	80	82	85.3	86.4	84.1	85.2	86.3	97.14
Recall	81.2	80.4	83.2	86.3	87.1	88.1	87.5	95.2
Specificity	82.3	81.4	79.4	86.4	88.4	86.5	87.2	98.4
FPR	0.31	0.38	0.15	0.1	0.1	0.1	0.1	0.015
FNR	0.18	0.23	0.11	0.13	0.13	0.13	0.13	0.047
AUC	70	73	80	81	86	87	89	93.33

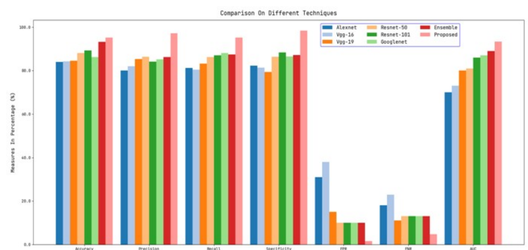

Figure 13: Comparison on different techniques

Table 9 and Figure 13 shows Comparative Analysis for various techniques in terms of Precision, Specificity, Recall, AUC,Accuracy, FPR and FNR. Based on the above comparison the proposed technique obtained optimal results in cervical cancer detection from Histopathological Images.Here the comparative analysis is carried put based on the tumor classes and their classification outputs. The proposed technique obtainPrecision of 97.14%,Specificity of 98.4%, Recall of 95.2%,AUC of 93.33%, Accuracy of 95.2%, FPR of 0.015% and FNR of 0.047%which is optimized when compared with existing techniques.

5. CONCLUSION

This paper proposed the novel technique in cervical cancer detection based on Histopathological images. To improve the efficiency, the network used to cluster the images using Optimal Kernelized Fuzzy C-Means clustering along with classified image to give high-resolution image classification.Then build an accurate cervical cancer Histopathological image ensemble based feature extraction model, which is the very first and most important procedure in our system. Depending on the pre-processed image, features are obtained are processed further for obtaining

ISSN: 1992-8645 www.jatit.org E-ISSN: 1817-3195

features which are not redundant because of the highest number of features, which are processable. Optimal Kernelized Fuzzy C-Means clustering method is classified using four classes i.e., NILM, SCC, LSIL and HSIL to optimize the results. The experimental result shows the comparison between proposed and existing techniques based on the parameters like Precision, Specificity, Recall, AUC,Accuracy, FPR and FNR. Thus this method reduces the cognitive burden on pathologists for cervical disease classification and improves their diagnostic efficiency and Accuracy.

REFERENCES:

[1] T. Muhammad, et al., “Classification of Colposcopy Data Using GLCM- SVM on Cervical Cancer”, *Proceedings of 2020 International Conference on Artificial Intelligence Information and Communication*. ICAIIC, 2020, pp. 373–378.

[2] Limming Hu, David Bell, Sameer Antani, Zhiyun Xue, et al., “An Observational Study of Deep Learning and Automated Evaluation of Cervical Images for Cancer Screening”, *Journal of the National Cancer Institute*, Vol. 111, No. 9, 2019, pp. 923–932.

[3] Masakazu Sato, Koji Horie, Aki Hara, Yuichiro Miyamoto, Kazuko Kurihara, Kensuke Tomia, Harushige Yokota, “Application of deep learning to the classification of images from colposcopy”, *Oncology Letters*, 2018, pp. 3518–3523. https://doi.org/10.3892/ol.2018.7762

[4] N. Dong, L. Zhao, C. H. Wu, and J. F. Chang, “Inception v3 based cervical cell classification combined with artificially extracted features”, *Applied Soft Computing,* Vol. 93, 2020, p. 106311.

[5] T. Zhang, Y. M. Luo, P. Li, et al., “Cervical precancerous lesions classification using pre-trained densely connected convolutional networks with colposcopy images”, *Biomedical Signal Processing and Control*, Vol. 55, 2020, p. 101566.

[6] P. Thakur and C. Lingam, “Generalized spatial kernel based fuzzy C-means clustering algorithm for image segmentation”, *International Journal of Science and Research (IJSR)*, Vol. 2, No. 5, 2013, pp. 165-169.

[7] A. Mahmood, M. Bennamoun, S. An, and F. Sohel, “Resfeats: Residual network based features for image classification”, *Proceedings of IEEE International Conference on Image processing (ICIP)*, September, 2017, pp. 1597-1601.

[8] J. Gao, J. Yang, G. Wang, and M. Li, “A novel feature extraction method for scene recognition based on centered convolutional restricted Boltzmann machines”, *Neurocomputing*, Vol. 214, 2016, pp. 708-717.

[9] T. I. Yusufaly, K. Kallis, A. Simon, et al., “A knowledge-based organ dose prediction tool for brachytherapy treatment planning of patients with cervical cancer”, *Brachytherapy*, Vol. 19, No. 5, 2020, pp. 624–634.

[10] J. Shao, Z. Zhang, H. Liu, et al., “DCE-MRI pharmacokinetic parameter maps for cervical carcinoma prediction”, *Computers in Biology and Medicine,* Vol. 118, No. C, 2020. https://doi.org/10.1016/j.compbiomed.2020.103634

[11] A. Ghoneim, G. Muhammad, and M. S. Hossain, “Cervical cancer classification using convolutional neural networks and extreme learning machines”, *Future Generation Computer Systems*, Vol. 102, 2020, pp. 643–649.

[12] J. Lu, E. Song, A. Ghoneim, and M. Alrashoud, “Machine learning for assisting cervical cancer diagnosis: an ensemble approach”, *Future Generation Computer Systems*, Vol. 106, pp. 2020, 199–205.

[13] S. I. Kim, S. Lee, C. H. Choi, M. Lee, J. W. Kim, and Y. B. Kim, “Prediction of disease recurrence according to surgical approach of primary radical hysterectomy in patients with early-stage cervical cancer using machine learning methods”, *Gynecologic Oncology*, Vol. 159, No. 2020, 2020, pp. 185-186.

[14] M. Nayak, S. Das, U. Bhanja, and M. R. Senapati, “Elephant herding optimization technique based neural network for cancer prediction”, *Informatics in Medicine Unlocked*, Vol. 21, Article 100445, 2020. DOI: 10.1016/j.imu.2020.100445

[15] V. Chandran, C. K. Patil, A. Karthick, D. Ganeshaperumal, R. Rahim, and A. Ghosh, “State of charge estimation of lithium - ion battery for electric vehicles using machine

learning algorithms", *World Electric Vehicle Journal*, Vol. 12, No. 1, 2021, p. 38.

[16] M. Suriya, V. Chandran, and M. G. Sumithra, "Enhanced deep convolutional neural network for malarial parasite classification", *International Journal of Computers and Applications*, 2019, pp. 1–10. DOI:10.1080/1206212X.2019.1672277

[17] A. Alghamdi, M. Hammad, H. Ugail et al., "Detection of myocardial infarction based on novel deep transfer learning methods for urban healthcare in smart cities", *Multimedia Tools and Applications*, 2020. https://doi.org/10.1007/s11042-020-08769-x

[18] Q. Meng, "Machine learning to predict local recurrence and distant metastasis of cervical cancer after definitive radiotherapy", *International Journal of Radiation Oncology*Biology*Physics*, Vol. 108, No. 3, Article e767, 2020. DOI: https://doi.org/10.1016/j.ijrobp.2020.07.208

[19] J. Shan, R. Jiang, X. Chen, et al., "Machine learning predicts lymph node metastasis in early-stage oral tongue squamous cell carcinoma", *Journal of Oral and Maxillofacial Surgery*, Vol. 78, No. 12, 2020, pp. 2208–2218.

[20] S. K. Saini, V. Bansal, R. Kaur, and M. Juneja, "ColpoNet for automated cervical cancer screening using colposcopy images", *Machine Vision and Applications*, Vol. 31, No. 3, 2020, pp. 1–15.

[21] P. Sanyal, P. Ganguli, and S. Barui, "Performance characteristics of an artificial intelligence based on convolutional neural network for screening conventional Papanicolaou-stained cervical smears", *Medical Journal, Armed Forces India*, Vol. 76, No. 4, 2020, pp. 418–424.

[22] B. R. Jany, A. Janas, and F. Krok, "Automatic microscopic image analysis by moving window local Fourier transform and machine learning", *Micron*, Vol. 130, Article 102800, 2020. https://doi.org/10.1016/j.micron.2019.102800